

## Evidence for a Commensurate-Incommensurate Phase Transition with an Intermediate Fluid Phase: N<sub>2</sub> Adsorbed on Ni(110)

M. Grunze, P. H. Kleban,<sup>(a)</sup> and W. N. Unertl<sup>(a)</sup>

*Fritz-Haber-Institut der Max-Planck-Gesellschaft, D-1000 Berlin 33, Federal Republic of Germany*

and

Franz S. Rys

*Institut für Festkörpertheorie der Freien Universität Berlin, D-1000 Berlin 33, Federal Republic of Germany*

(Received 2 November 1982)

Low-energy electron diffraction and thermodynamic measurements are reported for molecular nitrogen weakly chemisorbed on a Ni(110) surface in the temperature region between 87 and 150 K. A commensurate (2×1) phase transforms with increasing coverage into a sequence of smoothly varying incommensurate solid structures via a liquid-like intermediate phase. This is apparently the first experimental example of the commensurate-fluid-incommensurate phase sequence in uniaxial systems predicted by several recent theories.

PACS numbers: 64.70.Kb, 68.40.+e

The nature of thermodynamic phases and phase transitions in two-dimensional (2D) systems are topics of intense current interest. In particular, several recent theoretical papers have studied the properties of the commensurate-solid-incommensurate-solid (CI) phase transition at finite temperatures.<sup>1,2</sup> The structure of an adsorbed solid phase is described in terms of adsorbate unit mesh vectors ( $\vec{b}_1, \vec{b}_2$ ); we denote the substrate unit mesh vectors by ( $\vec{a}_1, \vec{a}_2$ ). For a commensurate phase the substrate unit mesh area is a rational fraction of the adsorbate unit mesh area; for an incommensurate phase it is not. In the special case of a rectangular substrate lattice ( $a_1 < a_2$ ) with a ( $p \times 1$ ) commensurate phase, i.e., ( $\vec{b}_1, \vec{b}_2$ ) = ( $p\vec{a}_1, \vec{a}_2$ ), the CI transition is predicted to occur in general via an intermediate fluid phase when  $p^2 < 8$ . In this Letter we report the first experimental observation of such a commensurate-fluid-incommensurate (CFI) phase sequence in a uniaxial system for molecular N<sub>2</sub> chemisorbed on a Ni(110) surface.<sup>3</sup>

There have been many extensive and thorough experimental studies of phase transitions in 2D physisorption systems. Studies of chemisorption systems, on the other hand, have (with several important exceptions<sup>4</sup>) generally focused on other properties. The work reported here provides an interesting new example of phase transitions in 2D chemisorption systems.

N<sub>2</sub> adsorption on Ni(110) is nondissociative for the temperatures and pressures employed (87–150 K, 10<sup>-11</sup>–10<sup>-5</sup> mbar). The N<sub>2</sub> molecule is weakly chemisorbed on top of the  $[\bar{1}10]$  Ni rows in a (at least on average) “standing up” configuration via the 3 $\sigma_g$  and 2 $\sigma_u$  orbitals of one nitrogen

atom.<sup>5</sup>

Figure 1 shows a schematic phase diagram for this system. The CFI transitions occur for N<sub>2</sub> coverages  $\theta$  between 0.5 monolayer and saturation. Below the dotted line, N<sub>2</sub> is irreversibly adsorbed and an N<sub>2</sub> background pressure is not required. Below the dot-dashed line, long relaxation times preclude equilibrium studies. The dashed line is an isobar recorded at the highest pressure accessible in the experiments, i.e.,  $p_{N_2} = 1.3 \times 10^{-6}$  mbar. Gas-adsorbate phase equilibrium measurements used to determine the thermodynamic data were performed in the  $T$ - $\theta$  region

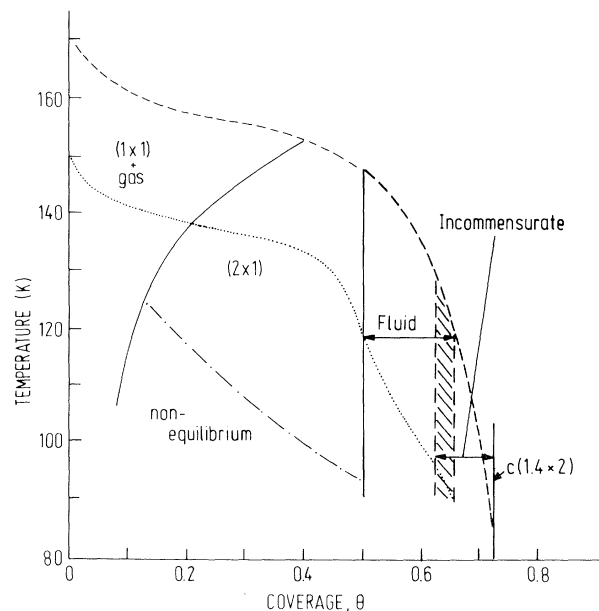


FIG. 1. Schematic phase diagram for N<sub>2</sub>/Ni(110).

between the dotted and dashed lines.

The experiments were carried out by use of low-energy electron diffraction (LEED), Auger-electron spectroscopy, thermal-desorption spectroscopy, and photoelectron spectroscopy. Excellent vacuum conditions are required since small amounts of  $H_2$  or CO significantly alter the results. Also, electron-beam-induced disordering and/or desorption limits the time available for measurements. A full account of the experimental procedures will be given elsewhere.<sup>6</sup>

$\theta$  was calibrated from relative variations in the  $N(1s)$  and  $Ni(2p)$  x-ray photoelectron intensities and from pressure rises during thermal-desorption measurements. The absolute coverage is  $\theta = 0.5 \pm 20\%$  [ $(0.57 \pm 0.12) \times 10^{15} N_2/cm^2$ ] for the sharpest  $(2 \times 1)$  LEED pattern [Fig. 2(b)].<sup>6</sup> Relative coverages were determined to within 2% from thermal-desorption data. These uncertainties in absolute coverage determination do not affect our conclusions.

Initial adsorption onto clean  $Ni(110)$  increases the LEED background intensity until a  $(2 \times 1)$  pattern appears. This pattern reaches maximum intensity, Fig. 2(b), near  $\theta = 0.5$ . Maximum ordering, as judged by the sharpness of the LEED beams, could only be achieved by annealing the sample briefly in  $N_2$  ( $p \sim 10^{-8}$  mbar,  $T \sim 125$  K). The real-space  $(2 \times 1)$  lattice is shown in Fig. 3(b). This  $(2 \times 1)$  structure is the most stable  $N_2$  phase on  $Ni(110)$  in this temperature range as it corresponds to the maximum heat of adsorption ( $\Delta H_{ad} = 47 \pm 7$  kJ/mole).<sup>6</sup>

Adsorption of  $N_2$  beyond  $\theta = 0.5$  produces "banana"-like features in the LEED pattern, Fig. 2(d), in which curved diffuse streaks connect  $\frac{1}{2}$ -order beams. The angular width of these diffuse streaks in a particular direction is inversely related to the coherence length  $\xi$  along that direction. Since the center of the curved part of each banana has a finite width,  $w$ , of about  $0.3 \text{ \AA}^{-1}$  along the  $[110]$  direction, there must be regions with  $\xi = 2\pi/w \approx 20 \text{ \AA}$ . In the  $[001]$  direction  $\xi$  has to be bigger, but determination of its exact value from LEED requires a structural model for the banana phase.

The banana structure forms rapidly (in times  $\leq 0.1$  sec) and reversibly from the  $(2 \times 1)$  phase along isobars as determined by the intensity of the  $\frac{1}{2}$ -order beams and by changes in the work function. By contrast, heating and cooling rates of less than  $0.05$  K/s and pressures greater than  $5 \times 10^{-8}$  mbar were required to obtain sharp LEED patterns and reversible work-function changes in

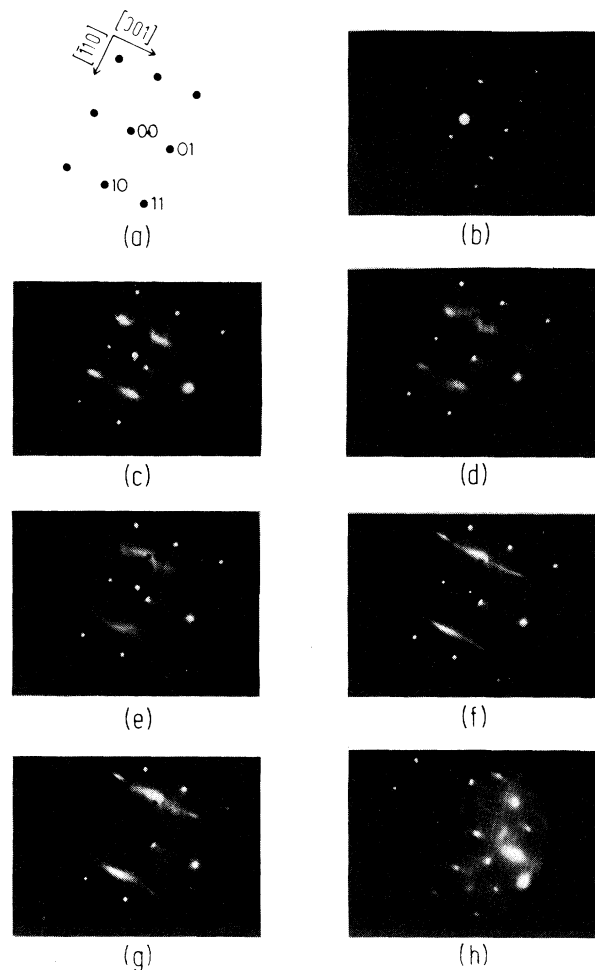


FIG. 2. (a) Schematic diffraction pattern for  $Ni(110)$  (Ref. 7). (b) The annealed  $(2 \times 1)$  pattern,  $\theta = 0.5$ , 87 eV. The patterns (c) to (g) were taken at 95 eV within  $2^\circ$  of normal incidence during an isobaric experiment at  $3 \times 10^{-7}$  mbar: (c) Diffuse  $(2 \times 1)$ ,  $\theta \approx 0.5$ ; (d) "banana,"  $\theta = 0.56$ ; (e) "banana,"  $\theta = 0.62$ ; (f)  $\theta = 0.68$ ; (g)  $\theta \approx 0.7$ ; (h)  $c(1.4 \times 2)$ , 88 K,  $p = 7 \times 10^{-6}$  mbar, incidence angle  $\approx 14^\circ$ , 88 eV.

the  $(2 \times 1)$  phase. Thus the kinetics of formation of the banana phase are at least two orders of magnitude more rapid than for the (fully developed)  $(2 \times 1)$ . Therefore we interpret the former to be a fluid rather than a solid with extensive frozen-in disorder. Note that the absence of slow kinetics also rules out the possibility that the banana is a fluid in coexistence with the  $(2 \times 1)$  phase, except perhaps in a very narrow range of coverages ( $\Delta\theta \approx 2\% \times 0.5 = 0.01 =$  experimental error).

A diffraction pattern similar to the banana pattern but without broadening can be produced by the simultaneous presence of structures whose

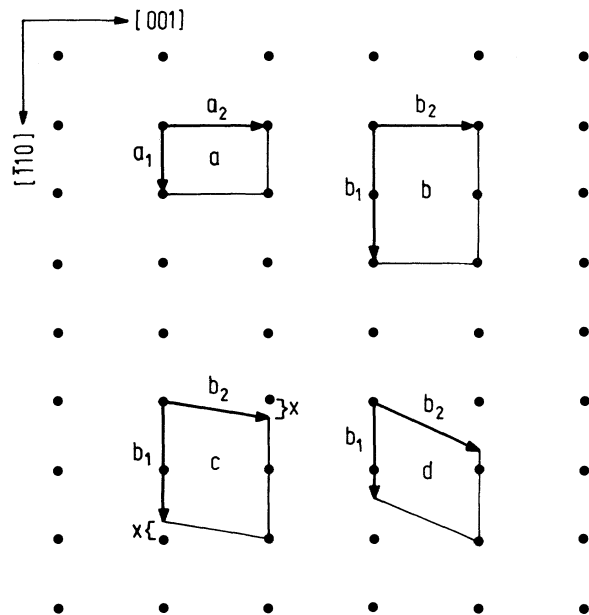


FIG. 3. Possible unit mesh adsorption structures discussed in the text. Dots represent the Ni(110)  $(1 \times 1)$  substrate lattice. There is one  $N_2$  in each overlayer mesh but its location cannot be determined without analysis of the diffracted intensities (Ref. 7). (a) The substrate unit mesh is defined by vector  $\vec{a}_1$  and  $\vec{a}_2$ . (b)  $(2 \times 1)$  unit mesh;  $\vec{b}_1 = 2\vec{a}_1$ ,  $\vec{b}_2 = \vec{a}_2$ . (c) Unit meshes which produce a diffraction pattern similar to the "banana" pattern, Figs. 2(d) and 2(e);  $\vec{b}_1 = (2-x)\vec{a}_1$  and  $\vec{b}_2 = x\vec{a}_1 + \vec{a}_2$  with  $0 < x < \frac{1}{2}$ . (d) Unit mesh for saturation structure  $c(1.4 \times 2)$ , Fig. 2(h);  $\vec{b}_1 = 1.4\vec{a}_1$  and  $\vec{b}_2 = 0.6\vec{a}_1 + \vec{a}_2$ . Observed structures evolve continuously from (b) to (d).

unit mesh vectors are given by  $\vec{b}_1 = (2-x)\vec{a}_1$  and  $\vec{b}_2 = x\vec{a}_1 + \vec{a}_2$ , where  $0 < x < \frac{1}{2}$ . Real-space meshes of this type are shown in Fig. 3(c); they all have one side  $\vec{b}_1$  of smoothly varying length and a range of registries between adjacent  $[110]$  rows. These meshes indicate the type of short-range order required to produce the banana structure.

In our picture of this fluid phase,  $N_2$  molecules are confined to move along  $[110]$  rows with average spacing inversely proportional to  $\theta$ . Interactions between adjacent rows are sufficiently strong to maintain some interrow correlation since for a one-dimensional fluid (i.e., no interrow interactions), the diffuse diffraction streaks would be straight rather than curved.

Further insight into the properties of this CF phase sequence is obtained from analysis of the entropies of adsorption, deduced from measured isosteric heats of adsorption.<sup>6</sup> The change in integral entropy from  $\theta \sim 0.5$ , where the banana phase is first observed, to  $\theta \sim 0.7$  is  $\Delta S \approx 20 \pm 10$

J/K mol ( $\approx 2.4 k_B$ /molecule). This large  $\Delta S$  is about two times the entropy of fusion of nitrogen<sup>8</sup> and cannot be due solely to translational degrees of freedom, since this would require an eleven-fold increase in the effective area per molecule. Therefore, new degrees of freedom must become available for  $\theta > 0.5$ .

Unfortunately, the order of the CF transition in the  $N_2/Ni(110)$  system cannot be determined from the present results. Some theories<sup>1</sup> suggest that the transition with low dislocation density is second order. On the other hand, a low dislocation core energy or domain-wall attraction could produce a first-order transition.<sup>9</sup> The large  $\Delta S$  might be thought to favor the latter. However, as shown above,  $\Delta S$  is much too large to be due only to translations. Furthermore, the shape and evolution of the LEED features in the banana phase and the lack of observed hysteresis are all consistent with a second-order transition of the predicted type. However, as noted above the experimental results by themselves do not rule out a coexistence between the banana and  $(2 \times 1)$  phases over a small region near the phase boundary.

As  $\theta$  increases further, the maximum intensity in each banana shifts from the  $\{\frac{1}{2}, 0\}$  positions of the  $(2 \times 1)$  phase toward  $\{\frac{2}{3}, \frac{1}{2}\}$  positions [Fig. 2(e)]. The LEED beams continue to evolve smoothly from the banana pattern into an incommensurate structure [Fig. 2(f)] which then compresses with increasing coverage until a  $c(1.4 \times 2)$  pattern is reached at the highest coverage accessible in these experiments [Figs. 2(g), 3(d)].  $N_2$  pressures greater than  $10^{-6}$  mbar and low temperatures are required to develop this structure fully. The diffraction beams sharpened first along the  $[110]$  direction and then along the  $[001]$  direction as the incommensurate structures developed. This stepwise evolution of beam shape indicates that anisotropic lateral interactions between adsorbed molecules play an important role. The work function and  $N(1s)$  photoelectron intensity varied reversibly and without hysteresis; LEED intensity measurements were not made. The smooth evolution of the diffraction pattern together with the thermodynamic data,<sup>6</sup> which show no change in the heat of adsorption to within  $\pm 3$  kJ/mole for  $0.55 < \theta < 0.72$ , suggest that there is no first-order phase transition between the banana and any of the incommensurate structures in this coverage range.

Near  $\theta \sim \frac{2}{3}$ , where an incommensurate structure is first observed, the LEED pattern is approxi-

mately described by the presence of symmetry-equivalent domains with unit mesh vectors  $\vec{b}_1 = \vec{a}_1 - \vec{a}_2$  and  $\vec{b}_2 = 2\vec{a}_1 + \vec{a}_2$ . Hence the observed pattern suggests a solidlike adsorbate structure. Occasionally one domain exhibits stronger intensity. Although all orders of this pattern are present, the beams were always diffuse indicating that a commensurate phase is not able to form with good long-range order. In fact, whether or not this structure, the  $c(1.4 \times 2)$ , or any other is in fact incommensurate with the substrate or coincides with it after a large number of unit meshes can never be unambiguously determined because of the finite resolution of any experiment.<sup>10</sup>

The possibility that the curved banana pattern is due to antiphase boundaries in either the  $(2 \times 1)$  or  $\theta = \frac{2}{3}$  phase can be ruled out since simple kinematical arguments show that additional diffraction features would be observed.

Thus, our LEED results indicate that the  $N_2/Ni(110)$   $(2 \times 1)$  commensurate phase melts to form a fluid phase before transforming into a sequence of incommensurate structures as the  $N_2$  coverage is increased from 0.5 to 0.72 monolayer. Theoretically, the fluid arises from an instability of the weakly incommensurate phase to free dislocations near the CF phase boundary.<sup>1</sup> For the present case, as  $\theta$  increases above one-half, the dislocations would be due to extra partial rows formed by the additional  $N_2$  molecules, on average in the  $[001]$  direction. Such dislocations could produce the banana diffraction pattern, if their strain fields fall off smoothly over  $\xi$ .

Our picture of the banana phase, described above, is fluidlike in the  $[\bar{1}10]$  direction and solidlike in the (perpendicular)  $[001]$  direction, with correlations between nearby  $[\bar{1}10]$  rows of adsorbed  $N_2$  molecules. Note that these features are consistent with a fluid of dislocations as predicted by theory.<sup>1</sup> The lack of translational symmetry of the banana pattern in the  $[\bar{1}10]$  direction (and its presence in the  $[001]$  direction) is also consistent with this part-fluid part-solid character. Finally, the fact that the banana pattern repeats in all visible (3 or 4) Brillouin zones in either direction<sup>5</sup> implies, in accord with theory, that there is a low density of dislocations; i.e.,

most of the  $N_2$  molecules are in or near  $(2 \times 1)$  positions. Detailed modeling of the banana structure will be presented elsewhere.<sup>11</sup>

This work was supported in part by the Deutsche Forschungsgemeinschaft, Sonderforschungsbereich 6, and by the U. S. Office of Naval Research. We thank J. H. Block, B. I. Halperin, and D. S. Fisher for helpful discussions.

<sup>(a)</sup>Permanent address: Department of Physics and Astronomy and Laboratory for Surface Science and Technology, University of Maine at Orono, Orono, Maine 04469.

<sup>1</sup>S. N. Coppersmith, D. S. Fisher, B. I. Halperin, P. A. Lee, and W. F. Brinkman, *Phys. Rev. Lett.* **46**, 549 (1981), and *Phys. Rev. B* **25**, 349 (1982); J. Villain and P. Bak, *J. Phys. (Paris)* **42**, 657 (1981).

<sup>2</sup>S. T. Chui, *Phys. Rev. B* **23**, 5982 (1981); M. Kardar and A. N. Berker, *Phys. Rev. Lett.* **48**, 1552 (1982); P. Bak and T. Bohr, to be published.

<sup>3</sup>The CFI sequence may also have been observed for CO adsorbed on Cu(110). [K. Horn, M. Hussain, and J. Pritchard, *Surf. Sci.* **63**, 244 (1977).] A sequence of LEED patterns similar to those shown in Fig. 2 was reported but without interpretation. See also the work of R. L. Gerlach and T. N. Rhodin, *Surf. Sci.* **10**, 446 (1968) for Na/Ni(110). A CFI sequence in a system with different symmetry has been reported by D. Moncton *et al.*, *Phys. Rev. Lett.* **46**, 1533 (1981).

<sup>4</sup>L. D. Roelofs, *Appl. Surf. Sci.* **11/12**, 425 (1982).

<sup>5</sup>M. Grunze, R. K. Driscoll, G. N. Burland, J. C. C. Cornish, and J. Pritchard, *Surf. Sci.* **89**, 381 (1979); K. Horn, J. DiNardo, W. Eberhard, H.-J. Freud, and E. W. Plummer, *Surf. Sci.* **118**, 465 (1982); J. Möller, W. N. Unertl, and W. Heiland, to be published.

<sup>6</sup>M. Golze, M. Grunze, R. K. Driscoll, and W. Hirsch, *Appl. Surf. Sci.* **6**, 464 (1980); M. Golze, M. Grunze, and R. K. Driscoll, to be published.

<sup>7</sup>The notation used here is described by D. P. Woodruff, in *The Chemical Physics of Solid Surfaces and Heterogeneous Catalysis*, edited by D. A. King and D. P. Woodruff (Elsevier, New York, 1981), Vol. 1.

<sup>8</sup>*Taschenbuch für Chemiker und Physiker*, edited by E. Lax and C. Synowietz (Springer-Verlag, Berlin, 1967), Vol. 1; K. Jones in *Comparative Inorganic Chemistry* (Pergamon, Oxford, 1973).

<sup>9</sup>Y. Saito, *Phys. Rev. Lett.* **48**, 1114 (1982); H. Kleinert, to be published.

<sup>10</sup>P. Bak, *Rep. Prog. Phys.* **45**, 587 (1982).

<sup>11</sup>P. Kleban, to be published.

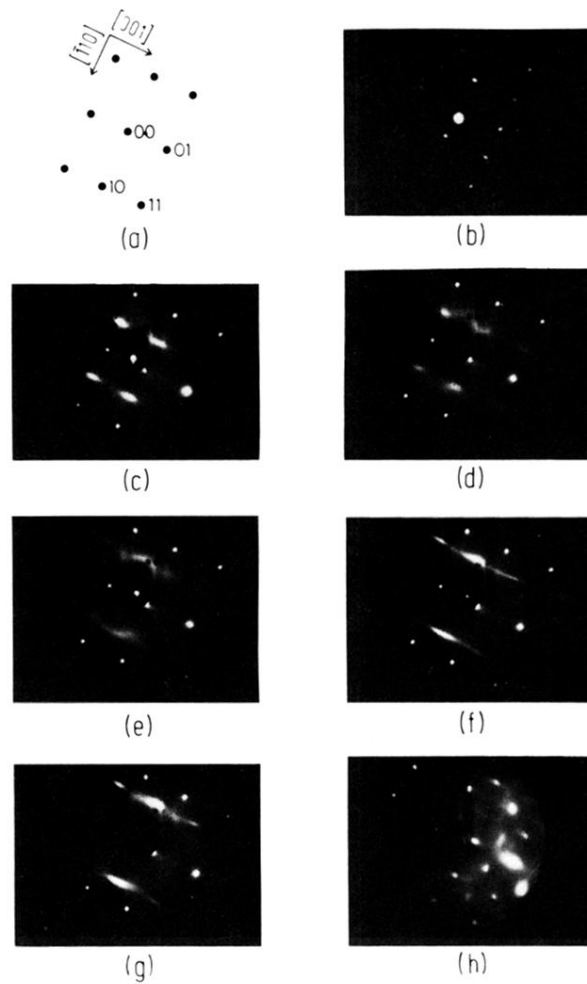


FIG. 2. (a) Schematic diffraction pattern for Ni(110) (Ref. 7). (b) The annealed  $(2 \times 1)$  pattern,  $\theta = 0.5$ , 87 eV. The patterns (c) to (g) were taken at 95 eV within  $2^\circ$  of normal incidence during an isobaric experiment at  $3 \times 10^{-7}$  mbar: (c) Diffuse  $(2 \times 1)$ ,  $\theta \approx 0.5$ ; (d) “banana,”  $\theta = 0.56$ ; (e) “banana,”  $\theta = 0.62$ ; (f)  $\theta = 0.68$ ; (g)  $\theta \approx 0.7$ ; (h)  $c(1.4 \times 2)$ , 88 K,  $p = 7 \times 10^{-6}$  mbar, incidence angle  $\approx 14^\circ$ , 88 eV.